Available online at www.sciencedirect.com
SCIENCE DIRECT®
European Journal of Medicinal Chemistry 39 (2004) 691–697
EUROPEAN JOURNAL OF MEDICINAL CHEMISTRY
www.elsevier.com/locate/ejmech

Original article

Studies on the synthesis and characterization of four *trans*-planaramineplatinum(II) complexes of the form *trans*-PtL(NH_3)CL_2 where L = 2-hydroxypyridine, 3-hydroxypyridine, imidazole, and imidazo(1,2-α)pyridine

Fazlul Huq [a,*], Hassan Daghriri [a], Jun Qing Yu [a], Philip Beale [b], Keith Fisher [c]

[a] *School of Biomedical Sciences, Cumberland Campus, C42, The University of Sydney, East Street, PO Box 170, Lidcombe, NSW 1825, Australia*
[b] *RPAH, Missenden Road, Camperdown, NSW, Australia*
[c] *School of Chemistry, F11, University of Sydney, NSW 2006, Australia*

Received 19 November 2003; accepted 30 April 2004

Abstract

Four *trans*-planaramineplatinum(II) complexes code named YH9, YH10, YH11 and YH12, each of the form *trans*-PtL(NH_3)Cl_2 where L = 2-hydroxypyridine and 3-hydroxypyridine, imidazole, and imidazo(1,2-α)pyridine for YH9, YH10, YH11 and YH12, respectively. All of the compounds have significant anticancer activity against human cancer cell lines. YH12 is found to be significantly more active than cisplatin against cisplatin-resistant ovary cell line $A2780^{cisR}$.

Keywords: Transplatin; Cisplatin; 2-Hydroxypyridine; 3-Hydroxypyridine; Imidazole; Anticancer activity

1. Introduction

Although cisplatin is a widely used anticancer drug that is highly effective against testicular and ovarian cancers and has proved beneficial in the treatment of head and neck, lung, and bladder cancers [1,2]; it has a number of side-effects including neurotoxicity, nephrotoxicity, ototoxicity, vomiting and hair-loss [3–7]. Also, cancer cells develop resistance to the continued use of cisplatin. In an attempt to reduce toxicity and widen the spectrum of activity, thousands of cisplatin analogues have been prepared and tested by varying the nature of the labile ligands (also called the leaving groups) and non-labile ligands (also called the carrier ligands). However, it is found that all cisplatin analogues generally have a similar spectrum of activity and develop similar resistance [8]. By manipulating the structure of the leaving groups it has been possible to reduce toxicity (e.g. substitution of the more stable cyclobutanedicarboxylate for the two chlorides led to the development of carboplatin which produces substantially less nausea, vomiting and neurotoxicity but causes more of myelosuppression), but it has not been possible to prevent cross resistance. It was hypothesized that the modification of the carrier ligands would change the spectrum of activity and indeed oxaliplatin which has 1,2-diaminocyclohexane as the carrier ligands and has been found to be active against colorectal cancer whilst cisplatin is not [9–11].

The reason why transplatin is toxic rather than being anticancer active is believed to be associated with its higher reactivity than cisplatin. It is, therefore, thought that the introduction of sterically hindered planar ligands may reduce the reactivity of the *trans*-complexes sufficiently so as to result into tumor-active compounds and because of different nature of binding with DNA with a spectrum of activity different from that of cisplatin [9]. One such class of compound is *trans*-planaramineplatinum(II) complexes. In general, transplatinum complexes with bulky planar ligands are found to be active in both murine and human cisplatin-resistant tumor cell lines [12].

* Corresponding author.
E-mail address: f.huq@fhs.usyd.edu.au (F. Huq).

doi:10.1016/j.ejmech.2004.04.005

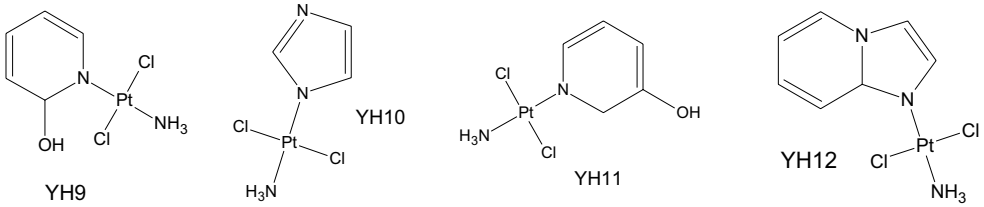

Fig. 1. Structures of four new *trans*-planaramineplatinun(II).

In this paper, we report the synthesis and spectral characterization of four *trans*-planaramine platinum(II) complexes of the type *trans*-$Pt(NH_3)LCl_2$ where L stands for 2-hydroxypyridine, 3-hydroxypyridine, imidazole and imidazo(1,2-α)pyridine (Fig. 1) and a brief overview of their anticancer activity. Detailed studies on anticancer activity of the compounds, their cell uptake, nature and extent of binding with DNA will be reported in a separate paper.

2. Materials and methods

2.1. Materials

Potassium tetrachloroplatinate $K_2[PtCl_4]$ and *N,N*-dimethylformamide [DMF] $[C_3H_7NO]$, 2-hydroxypyridine, 3-hydroxypyridine, imidazole and imidazo(1,2-α)pyridine were obtained from Sigma Chemical Company, St. Louis, USA; acetone ($(CH_3)_2CO$) and silver nitrate ($AgNO_3$) were obtained from Ajax Chemicals, Auburn, NSW, Australia; methanol (CH_3OH) and ethanol (C_2H_5OH) were obtained from Merck Pty. Limited, Kilsyth, Vic., Australia.

2.1.1. Syntheses

Trans-(2-hydroxypyridine)(ammine)dichloroplatinum(II) [code named YH9], *trans*-(imidazole)(ammine)dichloroplatinum(II) [code named YH10], *trans*-(3-hydroxypyridine)(ammine)dichloroplatinum(II) [code named YH11] and *trans*-{imidazo(1,2-α)pyridine}(ammine)dichloroplatinum (II) [code named YH12] were synthesized from potassium tetrachloroplatinate (K_2PtCL_4) according to Kauffman and Cowan [13] method shown in Fig. 2.

2.1.1.1. Cisplatin. Cisplatin, used as the starting material for the synthesis of the compounds, was prepared according to the modified Dhara [14] method. Briefly, the method was as follows. One millimol of tetrachloroplatinate was dissolved in 5 ml of milliQ (mQ) water. Potassium iodide (4.12 mmol), dissolved in 1 ml of mQ water, was added to the solution of potassium tetrachloroplatinate. The mixture was left on a shaking water bath at 37 °C for 5 min to produce K_2PtI_4 which was then reacted with 2 mmol of aqueous ammonia at 37 °C for 1 h to form *cis*-$Pt(NH_3)_2I_2$. The dark yellow precipitate was collected, washed with water and then with ice cold ethanol. It was then air dried. Silver nitrate (2 mmol) and *cis*-$Pt(NH3)_2I_2$ were mixed together followed by the addition of 4 ml of mQ water to the mixture. The mixture was left on a shaking water bath at 37 °C for 30 min to produce *cis*-$Pt(NH_3)_2(NO_3)_2$ and solid silver iodide. The mixture was centrifuged. The supernatant consisting of *cis*-$Pt(NH_3)_2(NO_3)_2$ in solution was collected. Potassium chloride (0.11 g, 1.5 mmol) was added to the solution and then the mixture was left on a water bath at 37 °C for 30 min for crystals of cisplatin to form. A brief description of syntheses of YH9, YH10, YH11 and YH12 is given below.

2.1.1.2. YH9. Cisplatin (0.3 g, 1 mmol) was added to 8 ml of mQ water. 2-Hydroxypyridine (0.19 g, 2 mmol), dissolved in a minimum amount of water, was added to cisplatin suspension. The mixture was heated at 70 °C with reflux for 1 h to cause 2-hydroxypyridine ligand replace the chloro ligands. The product was cooled to room temperature to stop the reaction. Concentrated HCl (1.22 ml, 12.2 mmol) was added to the mixture followed by heating to 70 °C with reflux to produce yellow needle shaped crystals of YH9. The crystals were collected at the pump, washed with mQ water and ice cold ethanol.

2.1.1.3. YH10. Cisplatin (0.3 g, 1 mmol) was dissolved in 8 ml of mQ water. Imidazole (0.136 g, 2 mmol), dissolved in a minimum amount of water, was added to the solution of cisplatin. The mixture was heated at 70 °C with reflux for 1 h to cause imidazole ligand replace the chloro ligands. The product was cooled to room temperature to stop the reaction. Concentrated HCl (1.22 ml, 12.2 mmol) was added followed by heating to 70 °C with reflux to produce yellow thin needle-shaped crystals of YH10. The crystals were collected at the pump, washed with mQ water and ice cold ethanol.

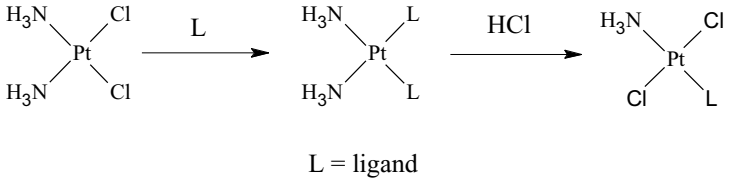

Fig. 2. Scheme for the syntheses of YH9, YH10, YH11 and YH12.

Table 1
Composition of YH9, YH10, YH11 and YH12

	YH9		YH10	
Molecular weight	378.11		350.08	
	Calculated (%)	Found (%)	Calculated (%)	Found (%)
C	15.9	16.0 ± 0.4	10.2S	10.9 ± 0.4
H	2.1	2.3 ± 0.4	1.73	2.0 ± 0.4
N	7.4	7.3 ± 0.4	12.0	11.8 ± 0.4
Cl	18.8	18.6 ± 0.3	20.2	20.2 ± 0.3
Pt	51.6	51.4 ± 1.2	55.7	55.1 ± 1.2
	YH11		YH12	
Molecular weight	378.11		401.15	
C	15.9	15.9 ± 0.4	21.0	22.0 ± 0.4
H	2.1	2.0 ± 0.4	2.3	2.6 ± 0.4
N	7.4	7.3 ± 0.4	10.5	10.5 ± 0.4
Cl	18.8	19.2 ± 0.3	17.7	17.3 ± 0.3
Pt	51.6	52.0 ± 1.2	48.5	48.1 ± 1.2

2.1.1.4. YH11. Cisplatin (0.3 g, 1 mmol) was added to 8 ml of mQ water. 3-Hydroxypyridine (0.19 g, 2 mmol), dissolved in 2 ml of ethanol (Huq and Yu, 2002), was added to the cisplatin suspension. The resulting mixture was heated at 70 °C with reflux for 1 h to cause 3-hydroxypyridine ligand replace the chloro ligands. The product was cooled to room temperature to stop the reaction. Concentrated HCl (1.22 ml, 12.2 mmol) was added followed by heating to 70 °C with reflux to produce thin yellow platy crystals of YH11. The crystals were collected at the pump, washed with mQ water and ice cold ethanol.

2.1.1.5. YH12. Cisplatin (0.3 g, 1 mmol) was added to 4 ml of mQ water. Imidazo(1,2-α)pyridine (0.2 ml, 2 mmol) was added to the cisplatin suspension. The mixture was heated at 70 °C with reflux for 1 h to cause the imidazo(1,2-α)pyridine ligand replace the chloro ligands. The product was cooled to room temperature to stop the reaction. Concentrated HCl (1.22 ml, 12.2 mmol) was added followed by heating to 70 °C with reflux to produce thin yellow platy crystals of YH12. The crystals were collected at the pump, washed with mQ water and ice cold ethanol. The compositions of YH9, YH10, YH11 and YH12 are given in Table 1.

2.1.2. Characterization

2.1.2.1. Microanalyses. C, H, N and Cl analyses were carried out using the facility at the Australian National University. Platinum content was determined by graphite furnace atomic absorption spectroscopy (AAS) using the Varian Spectraa-20 Atomic Absorption Spectrophotometer available in the School of Biomedical Sciences, The University of Sydney. Infrared spectra were collected using a Bruker IFS66 spectrometer equipped with a Spectra-Tech diffuse reflectance accessory (DRA), an air-cooled DTGS detector, a KBr beamsplitter with a spectral range of 4000–400 cm^{-1}. The instrument was run under a vacuum during spectral acquisition. Spectra were recorded at a resolution of 4 cm^{-1}, with the co-addition of 128 scans and a Blackman–Harris 3-Term apodization function was applied. Prior to analysis the samples were mixed, and lightly ground, with finely ground spectroscopic grade KBr. The spectra were then manipulated using the Kubelka–Munk mathematical function in the OPUS™ software to convert the spectra from reflectance into absorbance. Raman spectra were collected using a Bruker RFS100 Raman spectrometer equipped with an air-cooled Nd:YAG laser emitting at a wavelength of 1064 nm, and a liquid nitrogen cooled germanium detector with an extended spectral band range of 3500–50 cm^{-1}. One hundred and eighty degree sampling geometry was employed. Spectra were recorded at a resolution of 4 cm^{-1}, with the co-addition of 100 scans at a laser power of 0.065 mW. A Blackman–Harris 4-Term apodization function was applied and the spectra were not corrected for instrument response. To obtain mass spectra, solutions of DH4Cl, DH5Cl, DH6Cl and DH7Cl, made in 10% DMF and 90% methanol, were sprayed into a Finnigan LCQ ion trap mass spectrometer in which fragmentation was produced by electrospray ionization (ESI). ^{1}H NMR spectra of DH4Cl, DH5Cl, DH6Cl and DH7Cl were recorded in dimethylsulfoxide-d_6 (DMSO-d_6) solution (except in the case of DH4Cl which was dissolved in deuterated DMF) in a Bruker AVANCE DPX 400 spectrometer. Spectra were referenced to internal solvent residues and were recorded at 300 K (±1 K).

2.1.2.2. Molar conductivities. The molar conductivity values of YH9, YH10, YH11 and YH12 in solution in 1:4 mixture of DMF and water at 298 K were determined using PW9506 digital conductivity meter. The conductivity values were measured at the concentrations: 0.5, 0.25, 0.1 and 0.01 mM. The molar conductivity (A) was calculated as $A = k/c$, where k is the conductivity and c is the concentration (Atkins, 1998). The molar conductivity values obtained were then plotted against concentration to determine the limiting values.

2.1.2.3. Cytotoxicity. Cytotoxicity of the compounds against human ovarian cancer cell lines: A2780, A2780^{cisR},

A2780^{ZD0473R}, the melanoma cell line: Me 10538 and the non-small lung cancer cell line: NCI-H460 was determined using MTT growth inhibition assay [15]. Briefly, between 5000 and 9000 cells were seeded into the wells of the flat-bottomed 96-well culture plate in 10% FCS/RPMI 1640 culture medium. The plate was then incubated for 24 h at 37 °C in a humidified atmosphere to allow them to attach. Platinum complexes were first dissolved in a minimum volume of DMF, then diluted to the required concentrations by adding mQ water and finally filtered to sterilize. A serial fivefold dilutions of the drugs ranging from 0.02 to 62.5 μM in 10% FCS/RPMI 1640 medium were prepared and added to equal volumes of cell culture in quadruplicate wells, then left to incubate under normal growth conditions for 72 h. The inhibition of the cell growth was determined using the MTT assay. Four hours after the addition of MTT (50 μl per well of 1 mg ml^{-1} MTT solution), the cells were dissolved in 150 μl of DMSO and read with a plate reader (Bio-Rad Model 3550 Microplate Reader). The IC_{50} values were obtained from the results of quadruplicate determinations of at least three independent experiments.

3. Results and discussion

3.1. Composition

The compositions of the compounds are given in Table 1. The differences between expected and observed values are found to be within the errors of the measurement except for the carbon content of YH12.

3.2. IR and Raman spectral analyses

The prominent bands observed in the IR and Raman spectra of YH9, YH10, YH11 and YH12 are given in Table 2.

3.2.1. YH9 [trans-*(ammine)(2-hydroxypyridine)dichloroplatinum(II)]*

3.2.1.1. IR. The broad band at 3289 cm^{-1} is believed to be due to N–H and O–H stretching vibrations, whereas that at 3064 is due to C–H stretch. The band at 1621 cm^{-1} is believed to be due to N–H bending vibration, whereas those at 1573 and 1484 cm^{-1} are believed to be due to the 'aromatic' ring stretching vibrations. The band at 1319 cm^{-1} is due to O–H bending vibration. The bands at 1172 and 1105 cm^{-1} are believed to be due to C–O stretch. The band at 781 is due to out-of-plane C–H bending vibration. The band at 547 and 514 cm^{-1} are believed to be due to Pt–N(NH_3) stretching vibrations, whereas that at 482 is associated with the vibration of pyridine ring.

3.2.1.2. Raman. The band at 3160 cm^{-1} is due to N–H and C–H stretching vibrations. The band at 1572 is due to N–H bending vibration. The bands at 1311, 1240, 1153 and 1034 cm^{-1} are believed to be due to C–H in-plane bending vibrations. The band at 1103 is due to C–O stretch. The band at 847 cm^{-1} is due to C–H out-of-plane bending. The band at 659 cm^{-1} is associated with the vibration of the pyridine ring. The bands at 517 and 573 cm^{-1} are due to Pt–N(NH_3) stretching vibrations. The band at 326 cm^{-1} is due to Pt–Cl stretching vibration. The bands at 193 and 237 cm^{-1} are due to Pt–N(2-hydroxypyridine) stretching vibrations. The band at 143 cm^{-1} is due to Pt–N bending vibration. The band at 81 cm^{-1} is believed to be associated with the lattice mode.

3.2.2. YH10 [trans-*(animine)(imidazole)dichloroplatinum (II)]*

3.2.2.1. IR. The broad band at 3280 cm^{-1} is believed to be due to N–H stretching vibration, whereas that at 3145 is believed to be due to C–H stretch. The bands at 1631 and

Table 2
Prominent IR Raman spectral bands observed in YH9, YH10, YH11 and YH12 (ν, cm^{-1})

	IR (cm^{-1})	Raman
YH9	3289 (s, NH and OH), 3064 (w, CH), 1621 (m, NH), 1573 (m, 'aromatic ring'), 1484 (s, 'aromatic ring'), 1319 (s, OH), 1172 (s, CO), 1105 (w, CO), 781 (s, CH), 547 (m, Pt–N), 514 (m, Pt–N), 482 (m, pyridine ring)	3160 (w, NH and CH), 1572 (w, NH), 1311 (w d, CH), 1240 (w, CH), 1153 (w, CH), 1034 (m, CH), 847 (s, CH), 659 (w, pyridine ring), 573 (w, Pt–N(NH_3)), 517 (w, Pt–N(NH_3)), 237 (w, Pt–N(2-hydroxypyridine)), 193 (w, Pt–N(2-hydroxypyridine)), 143 (s, Pt–N), 81 (m, lattice)
YH10	3280 (s, NH), 3145 (m, CH), 1697 (w, C=C and NH), 1631 (w, C=C and NH), 1542 (m, C=N), 1311 (s, imidazole ring), 844 (m, imidazole ring), 844 (m, CH and NH), 755 (s, CH and NH), 709 (m, CH), 653 (m, CH), 614 (s, CH and NH)	3151 (w,NH), 1782 (w br, 'aromatic' CH overtone), 1431 (w, CN), 1331 (w, CH), 1263 (w, NH), 1186 (w, NH), 1138 (w, NH), 524 (w, Pt–N), 326 (m, Pt–Cl), 249 (w, Pt–N(imidazole)), 222 (w, imidazole), 133 (Pt–N)
YH11	3261 (s br, NH and OH), 3077 (w, CH), 2562 (w, pyridine ring), 2447 (w, pyridine ring), 2141 (w, pyridine ring), 1887 (w, pyridine ring), 1610 (w, NH), 1579 (m, NH), 1315 (s, OH), 1224 (s, CO), 869 (m, CH), 802 (s, CH), 688 (m, pyridine ring), 593 (s, Pt–N(NH_3)), 545 (m, Pt–N(NH_3)), 518 (m, Pt–N(NH_3)), 441 (w, pyridine ring)	3253 (w br, NH and OH), 3190 (w br, NH and OH), 3099 (w, CH), 3074 (w, CH), 1618 (w, pyridine ring), 1577 (w, NH), 1469 (w, NH), 1321 (w, OH), 1279 (w, CH), 1176 (w, CH), 1109 (w, CO), 1030 (s, CH), 870 (m, CH), 655 (w, CH), 523 (m, Pt–N), 442 (w, Pt–N), 345 (m, Pt–Cl), 316 (m, Pt–Cl), 243 (m, Pt–N(3-hydroxypyridine)), 187 (w, Pt–N), 91 (s, Pt–N), 67 (s, lattice)
YH12	3243 (m br, NH), 3243 (m br, NH), 3133 (m br, CH), 1637 (m, ring stretch), 1511 (s, ring stretch), 1446 (w, ring stretch), 1320 (s, ring), 1234 (w, C–N), 1149 (w br, C–N), 838 (w, ring), 752 (s, CH), 725 (m, CH), 447 (m, Pt–N), 422 (s, Pt–N)	3120 (w, NH), 3082 (w, CH), 1635 (w, ring), 1512 (m, ring), 1377 (w, ring), 1321 (m,NH), 1234 (w, NH), 1132 (w, NH), 1012 (w, CH), 887 (w, CH), 771 (w, CH), 638 (w, CH), 569 (w, P–N), 328 (m, Pt–Cl), 239 (w, Pt–N(ring), 100 (Pt–N)

1697 cm^{-1} are believed to be due to C=C stretching and N–H bending vibrations. The band at 1542 cm^{-1} is believed to be due to C=N stretch. The band at 1311 cm^{-1} is due to in-plane deformation of the imidazole ring, whereas that at 844 is due to its out-of-plane deformation. The bands at 1182 and 1141 cm^{-1} are due to C–H in-plane bending vibrations. The bands at 844, 755, 709, 653 and 614 cm^{-1} are believed to be due to out-of-plane bending of the ring C–H and N–H bonds.

3.2.2.2. Raman. The band at 3151 is due to N–H stretching vibration. The band at 1782 cm^{-1} is believed to be an overtone band associated with 'aromatic' C–H stretch. The band at 1541 cm^{-1} is believed to be due to 'aromatic' C=C and C=N stretching vibrations. The band at 1431 cm^{-1} is believed to be due to C–N stretch. The band at 1331 cm^{-1} is due to in-plane bending of the C–H bond. The bands at 1263, 1186 and 1138 cm^{-1} are believed to be due to N–H bending vibrations. The band at 524 cm^{-1} is due to Pt–N stretching vibration, whereas that at 326 is due to Pt–Cl stretching vibration. The bands at 222 and 249 cm^{-1} are due Pt–N(imidazole) stretching vibrations, whereas that at 133 cm^{-1} is due to Pt–N bending vibration.

*3.2.3. YH11 [*trans-*(ammine)(3-hydroxypyridine)dichloroplatinum(II)]*

3.2.3.1. IR. The broad band at 3261 cm^{-1} is believed to be due to N–H and O–H stretching vibrations, whereas that at 3077 is due to C–H stretch. The bands at 2562, 2447, 2141 and 1887 cm^{-1} are associated with the vibrations of 3-hydroxypyridine ring. The bands at 1610 and 1579 cm^{-1} are due to N–H bending vibrations. The band at 1224 cm^{-1} is believed to be due to C–O stretching vibration. The band at 1315 cm^{-1} is believed to be due to in-plane O–H bending. The bands at 869, 802 and 688 cm^{-1} are believed to be associated with the out-of-plane bending of the ring C–H bonds. The band at 688 cm^{-1} applies to the in-plane deformation of the pyridine ring, whereas that at 441 cm^{-1} applies to its out-of-plane deformation. The bands at 518, 545 and 593 cm^{-1} are believed to be due to Pt–N(NH_3) stretching vibrations.

3.2.3.2. Raman. The bands at 3253 and 3190 cm^{-1} are due to O–H and N–H stretching vibrations. The bands at 3099 and 3074 are due to C–H stretch. The bands at 1618 cm^{-1} is associated with the vibration of 3-hydroxypyridine ring. The bands at 1577 and 1469 cm^{-1} are believed to be due to N–H bending vibrations. The band at 1321 cm^{-1} is due to O–H bending vibration. The bands at 1279 and 1176 cm^{-1} are believed to be due to C–H in-plane bending vibrations. The band at 1109 cm^{-1} is due to C–O stretch. The band at 1030 cm^{-1} is due to C–H in-plane bending of the hetereocyclic ring. The bands at 870 and 655 cm^{-1} are believed to be due to C–H out-of-plane bending. The bands at 523 and 442 is due to Pt–N(NH_3) stretching vibrations, whereas that at 345 cm^{-1} is due to Pt–Cl stretching vibration. The band at 243 is due Pt–N(3-hydroxypyridine) stretching vibration. The bands at 189 and 91 cm^{-1} are believed to be due to Pt–N bending vibrations. The band at 67 cm^{-1} is associated with the lattice mode.

*3.2.4. YH12 [*trans-*(ammine)(imidazo(1,2-α)pyridinato)dichloroplatinum(II)]*

3.2.4.1. IR. The bands at 3299 and 3243 cm^{-1} are believed to be due to symmetric and asymmetric NH_3 stretch and that at 3133 cm^{-1} is due to C–H stretch. The bands 1637, 1511, 1446 and 1320 cm^{-1} are believed to be due to ring stretch. The band at 1542 cm^{-1} is due to C=C stretch. The band at 1320 cm^{-1} is due to in-plane deformation of the imidazole ring, whereas that at 838 is due to its out-of-pane deformation. The bands 1149 and 1234 cm^{-1} are believed to be due to C–N stretching vibrations. In the free ligand, the corresponding bands appear at 1150 and 1250 cm^{-1}. The bands at 752 and 725 cm^{-1} are believed to be due to C–H out-of-plane bending vibrations. The bands at 422 and 447 cm^{-1} are believed to be due to Pt–N(NH_3) stretching vibrations.

3.2.4.2. Raman. The band at 3120 cm^{-1} is believed to be due to N–H stretching vibration, whereas that at 3082 is due to C–H stretch. The bands at 1635, 1512 and 1337 cm^{-1} are believed to be due to ring stretch. The bands at 1321, 1234 and 1132 cm^{-1} are believed to be due to N–H bending vibrations. The band at 1012 cm^{-1} is due to C–H in-plane bending of the heterocyclic ring. The bands at 887, 771 and 638 cm^{-1} are believed to be due to C–H out-of-plane bending. The band at 569 cm^{-1} is due to Pt–N(NH_3) stretching vibration, whereas that at 328 cm^{-1} is due to Pt–Cl stretching vibration. The band at 239 cm^{-1} is due Pt–N(ring) stretching vibration, whereas that at 100 cm^{-1} is due to Pt–N(NH_3) bending vibration.

3.3. Mass ^{1}H NMR spectral analyses

The prominent peaks observed in the ESI mass and ^{1}H NMR spectra of YH9, YH10, YH11 and YH12 are given in Table 3.

3.3.1. YH9

3.3.1.1. Mass spectrum. The mass spectrum of YH9 has a peak with *m/z* = 377 that corresponds to (M – H), that at 360 corresponds to (M – H – NH_3), that at 339 corresponds to (M – Cl – 4H) and at 324 corresponds to (M – Cl – NH_3 – 2H).

3.3.1.2. ^{1}H NMR. The resonance at δ = 12.07 ppm is believed to be due to OH proton. The resonance at δ = 8.28 ppm is due to *ortho* CH proton and that at δ = 8.27 ppm is due to CH proton adjacent to the carbon to which OH group is attached. The resonance at δ = 7.70 ppm is due to CH proton at the *para* position and that at δ = 6.85 ppm is due to CH proton at the

Table 3
The mass spectra of YH9, YH10, YH11, and YH12 where the number in parentheses after each *m/z* value indicates the relative intensity

	ESI mass (*m/z*)	^{1}H NMR
YH9	ESI-MS (DMF) (M – H) = 377 (0.17); (M – Cl – 4H) = 339 (1.00);(M – Cl – NH_3 – 2H) = 324 (0.69)	^{1}H NMR DMSO 6 ppm: 12.07 (s, due to OH); 8.28; 7.85 (t, ?); 7.70 (quartet, due to CH *para*); 6.85 (quartet, CH *meta*); 4.60 (s, due to NH–Pt); 3.86 (d, due to NH–Pt); 3.34 (s, due to water); 2.50 (due to DMS)
YH10	ESI-MS (DMF) (Pt(imidazole)$_3$Cl = 433 (0.38); (M – Cl + imidazole) = 384; (M – NH_3 – 2H) = 332 (0.07))	^{1}H NMR DMSO 8 ppm: 8.35 (s, due to NH); 8.09 (s, due to CH); 7.42 (s, due to CH); 7.24 (s, ?); 7.20 (s, due to CH); 4.60 (s, due to NH–Pt); 3.76 (d, due to NH–Pt); 3.32 (s, due to water); 2.50 (due to DMS)
YH11	EIS-MS (DMF) (PtCl(3-hydroxypyridine)$_3$ = 516 (0.36); (M – Cl + 3-hydroxypyridine) = 438 (1.00) ;(M – H) = 377 (0.09); (M – H – NH_3) = 360; (M – Cl – NH_3 – H) = 324 (0.66); (M – Cl – 3-hydroxypyridine + NH_3) = 265 (0.31)	^{1}H NMR DMSO 5 ppm: 10.80 (s, due to OH); 8.32 (s, due to CH *ortho*); 8.30 (due to CH); 8.26 (d, due to CH); 7.33 (quartet, due to CH); 6.85 (quartet, CH *meta*); 4.60 (s, due to NH–Pt); 3.90 (d, due to NH–Pt); 3.32 (s, due to water); 2.50 (due to DMS)
YH12	ESI-MS (DMF) ((PtCl {imidazo(1,2-α)pyridine}$_3$-H) = 584 (0.22); Pt(NH_3)(imidazo(1,2-α)pyridine)$_2$Cl = 484 (1.00); Pt (imidazo(1,2-α)pyridine)2 = 431 (0.04); M – NH_3 – H = 383 (0.09); $PtCl_3$ = 301 (0.59))	^{1}H NMR DMSO 8 ppm: 8.73 (d, due to CH); 8.61 (d, due to CH); 8.19 (d, due to CH); 8.03 (quartet, due to CH); 7.70 (quartet, due to CH); 4.60 (s, due to NH–Pt); 3.96 (d, due to NH–Pt); 3.34 (s, due to water); 2.50 (due to DMS)

second *meta* position. The resonance at $\delta = 4.60$ ppm is due to NH bonded to Pt. Likewise, the resonance at $\delta = 3.86$ ppm is believed to be due to NH bonded to Pt. The resonance at $\delta = 3.34$ ppm is due to water and that at $\delta = 2.50$ ppm is due to DMSO.

3.3.2. YH10

3.3.2.1. Mass spectrum. The mass spectrum of YH10 has a peak with *m/z* = 384 that corresponds to Pt(imidazole)$_3$(NH_3)Cl that is believed to be formed in situ from the joining of fragments produced from YH10. The peak with *m/z* = 332 corresponds to (M – 2H – NH_3).

3.3.2.2. ^{1}H NMR. The resonance at $\delta = 8.35$ ppm is due to NH proton and that at $\delta = 8.09$ ppm is due to *ortho* CH proton that lies in between the two nitrogens. The resonance at $\delta = 7.42$ ppm is due to the other *ortho* CH proton and that at $\delta = 7.20$ ppm is due to CH proton at the *meta* position. It is difficult to explain why there is an additional proton resonance at 7.24 ppm unless it is assumed that the nitrogen at the third position is protonated. It is interesting to note that the NH resonance has shifted from 13.4 ppm in pure imidazole to 8.35 ppm in the Pt-complex. The resonance at $\delta = 4.60$ ppm is due to NH bonded to Pt. Likewise, the resonance at $\delta = 3.76$ ppm is believed to be due to NH bonded to Pt. The resonance at $\delta = 3.32$ ppm is due to water and that at $\delta = 2.50$ ppm is due to DMSO.

3.3.3. YH11

3.3.3.1. Mass spectrum. The mass spectrum of YH11 has a peak with *m/z* = 516 that corresponds to PtCl(3-hydroxypyridine)$_3$ that is believed to be formed in situ from the joining of fragments produced from YH11. The peak with *m/z* = 438 is believed to be due to (M – Cl + 3-hydroxypyridine), that at 377 corresponds to (M – H), that at 360 corresponds to (M – H – NH_3), that at 324 corresponds to (M – Cl – NH_3 – 2H) and that at 265 corresponds to (M – Cl – 3-hydroxypyridine + NH_3). It can be seen that although the mass spectra of YH9 and YH11 differ significantly, both the spectra have peaks at 377 and 360 corresponding to (M – H) and (M – H – NH_3).

3.3.3.2. ^{1}H NMR. The resonance at $\delta = 10.90$ ppm is believed to be due to OH proton. The resonance at $\delta = 8.32$ ppm is due to H attached to the second carbon and that at $\delta = 8.30$ ppm is due to H attached to the sixth carbon. The resonance at $\delta = 8.26$ ppm is due to H attached to the fourth carbon and that at $\delta = 7.33$ ppm is due to H attached to the fifth carbon. The resonance at $\delta = 4.60$ ppm is due to NH bonded to Pt. Likewise, the resonance at $\delta = 3.90$ ppm is believed to be due to NH bonded to Pt. The resonance at $\delta = 3.31$ ppm is due to water and that at $\delta = 2.50$ ppm is due to DMSO.

3.3.4. YH12

3.3.4.1. Mass spectrum. The mass spectrum of YH12 has a peak with *m/z* = 584 that corresponds to {PtCl{imidazo(1,2-α)pyridine)$_3$-H} that is believed to be formed in situ from the joining of fragments produced from YH12. The peak with *m/z* = 484 is believed to be due to PtCl(NH_3){imidazo(1,2-α)pyridine)$_2$} that is believed to be formed in situ from the joining of fragments produced from YH12. The peak with *m/z* = 383 corresponds to (M – H – NH_3), that at 324 corresponds to (M – Cl – NH_3 – H) and that at 301 is due to $PtCl_3$.

3.3.4.2. ^{1}H NMR. The resonance at $\delta = 8.73$ ppm is due to H attached to the second carbon and that at $\delta = 8.61$ ppm is due to H attached to the third carbon. The resonance at $\delta = 8.19$ ppm is due to H attached to the ninth carbon and that at $\delta = 8.03$ ppm is due to H attached to the eighth carbon. The resonance at $\delta = 7.70$ ppm is due to H attached to the seventh carbon. The resonance at $\delta = 4.60$ ppm is due to NH bonded to Pt. Likewise, the resonance at $\delta = 3.96$ ppm is believed to be due to NH bonded to Pt. The resonance at $\delta = 3.34$ ppm is due to water and that at $\delta = 2.50$ ppm is due to DMSO.

Table 4
IC_{50} value and resistance factors for cisplatin, YH9, YH10, YH11 and YH12

	A2780 IC_{50}	A2780-cisR IC_{50}	$IC_{50}A2780^{cisR}/IC_{50}A2780$ RF	$A2780^{ZD0473R}$ IC_{50}	NCI-H460 IC_{50}	Me 10538 IC_{50}
Cisplatin	0.45 ± 0.1	4.43 ± 0.1	9.9	2.15 ± 0.6	1.15 ± 0.2	3.40 ± 0.6
YH9	14.88 ± 8.1	18.52 ± 13.5	1.2	10.92 ± 1.1	44.67 ± 6.8	26.25 ± 2.3
YH10	13.24 ± 1.5	16.52 ± 3.44	1.3	17.86 ± 3.5	38.96 ± 4.4	23.00 ± 2.3
YH11	11.70 ± 1.9	14.98 ± 2.1	1.3	16.18 ± 1.6	33.78 ± 4.6	19.99 ± 2.7
YH12	4.40 ± 1.6	2.34 ± 0.5	0.5	4.87 ± 0.3	9.16 ± 2.0	8.12 ± 1.3

3.3.4.3. Molar conductivity values. The limiting values of molar conductivity (in ohm^{-1} cm^2 mol^{-1}) at zero concentration of YH9, YH10, YH11 and YH12 at 298 K were found to be 78, 78, 102 and 132, respectively. These values are significantly lower than the expected values of about 280 for 1:2 electrolyte, indicating that the degree of dissociation is of the order of about 30% in the case of YH9, YH10 and YH11 and about 50% in the case of YH12.

These results suggest that the compounds may be crossing the cell membrane by both passive diffusion and carrier-mediated transport.

3.3.4.4. Cytotoxicity. Table 4 gives the IC_{50} values of cisplatin, YH9, YH10, YH11 and YH12 against the cell lines: A2780, $A2780^{cisR}$, $A2780^{ZD0473R}$, Me 10538 and NCI-H460. All of the compounds are found to be less active than cisplatin against all the cell lines except YH12 which is found to be twice as active as cisplatin against the cell line: $A2780^{cisR}$, indicating that YH12 has been able to overcome mechanisms of resistance operating in the cell line. The variations in activity of the compounds illustrate structure–activity relationship.

Acknowledgements

The authors are thankful to Dr. Ian Luck of School of Chemistry, The University of Sydney for his assistance in recording ^1H NMR spectra. Jun Qing Yu is thankful to the University of Sydney for a UPA.

References

[1] H.M. Pinedo, J.H. Schornagel, Platinum and Other Metal Coordination Compounds in Cancer Chemotherapy, 2, Plenum Press, New York, 1996.
[2] P.J. Loehrer, L.H. Einhorn, Ann. Intern. Med. 100 (1984) 704–713.
[3] R.T. Dorr, W.L. Fritz, Cancer Chemotherapy Handbook, Kimpton, London, 1980.
[4] A.H. Calvert, D.R. Newell, M.J. Tilby, Oxford Textbook of Oncology, Oxford University Press, Oxford, New York, 1995.
[5] G.A. Daugaard, U. Abildgaard, Chemother. Pharmacol. 25 (1989) 1–9.
[6] M.J. Moroso, R.L. Blair, J. Otolaryngol. 12 (1983) 365–369.
[7] L.X. Cubeddu, I.S. Hoffmann, N.T. Fuenmayor, A.L. Finn, New Engl. J. Med. 322 (1990) 810–816.
[8] A. Gelasco, S. Lippard, Metallopharmaceuticals I: DNA Interactions, Springer, Berlin, London, 1999.
[9] N. Farrell, Met. Ions Biol. Syst. 32 (1996) 603–639.
[10] G. Natile, M. Coluccia, Metallopharmecuticals I: DNA Interactions, Springer, Berlin, London, 1999.
[11] F. Levi, B. Perpoint, C. Focan, P. Chollet, P. Depres-Brummer, R. Zidani, S. Brienza, M. Itzhaki, S. Iacobelli, et al., Eur. J. Cancer 29A (1993) 1280–1284.
[12] N. Farrel, L.R. Kelland, J.D. Roberts, M. Van Beusichem, Cancer Res. 52 (1992) 5065–5072.
[13] G. Kauffman, D. Cowan, Inorg. Synth. 7 (1963) 239–245.
[14] S. Dhara, Indian J. Chem. 8 (1970) 193–194.
[15] T. Mosmann, J. Immunol. Methods 65 (1983) 55–63.